Endothelial damage and dysfunction in acute graft-*versus*-host disease

Steffen Cordes,[1] Zeinab Mokhtari,[2] Maria Bartosova,[3] Sarah Mertlitz,[1] Katarina Riesner,[1] Yu Shi,[1] Jörg Mengwasser,[1,4] Martina Kalupa,[1] Aleixandria McGeary,[1] Johanna Schleifenbaum,[5,6] Jens Schrezenmeier,[1] Lars Bullinger,[1] Maribel Diaz-Ricart,[7] Marta Palomo,[7,8] Enric Carreras,[8] Gernot Beutel,[9] Claus Peter Schmitt, [3]Andreas Beilhack[2] and Olaf Penack[1]

[1]Department of Hematology, Oncology and Tumor Immunology, Charité Universitätsmedizin Berlin, Campus Virchow Clinic, Berlin, Germany; [2]Department of Medicine II, Würzburg University Hospital, Interdisciplinary Center for Clinical Research (IZKF), Laboratory for Experimental Stem Cell Transplantation, Würzburg, Germany; [3]Pediatric Nephrology, Center for Pediatric and Adolescent Medicine, University Hospital Heidelberg, Heidelberg, Germany; [4]Department of Surgery, Charité Universitätsmedizin Berlin, Campus Charité Mitte/Campus Virchow Clinic, Berlin, Germany; [5]Experimental and Clinical Research Center (ECRC) - a joint cooperation between the Charité Medical Faculty and the Max Delbrück Center for Molecular Medicine (MDC), Berlin, Germany; [6]Charité Universitätsmedizin Berlin, Institute of Vegetative Physiology, Berlin, Germany; [7]Department of Hematopathology, Hospital Clinic of Barcelona, Biomedical Diagnosis Centre (CDB), Institute of Biomedical Research August Pi i Sunyer (IDIBAPS), University of Barcelona, Barcelona, Spain; [8]Josep Carreras Leukemia Research Institute, Hospital Clinic/University of Barcelona Campus, Barcelona, Spain and [9]Department of Hematology, Hemostasis, Oncology and Stem Cell Transplantation, Hannover Medical School, Hannover, Germany

Summary of Methods used in the main manuscript

Patient material and histology of human biopsies

Collection of human samples was approved by the institutional ethics committees of Charité Berlin and Medical University Hannover and was in accordance with the Declaration of Helsinki. Intestinal biopsies were collected from patients with suspected intestinal aGVHD after written informed consent was obtained. From the Charité cohort, we included intestinal biopsies with aGVHD versus no aGVHD after allo-HSCTs performed between 2007 and 2015. We identified 12 duodenal and 11 colon biopsies from patients with aGVHD grade III-IV. As a control, we used 19 duodenal and 10 colon biopsies from allo-HSCT recipients without histological evidence of aGVHD.[1] From the Hannover cohort colon biopsies from 11 patients with aGVHD were included. From each patient, biopsies were taken at two time points: at diagnosis of aGVHD and later at diagnosis of SR-aGVHD. Detailed clinical data from both cohorts are given in supplementary tables 1-2 and 4-6.

Immunohistochemistry was performed on formalin fixed tissue sections. After blocking (3% H_2O_2) and heat-induced antigen retrieval (citrate buffer, pH6 from Dako Cytomation, Glostrup, Denmark) primary anti-cleaved caspase 3 antibody (Casp3 from Cell Signaling, Asp175, 1:1000) was applied. Anti-CD45 and anti-CD3 staining was done in the Charité core facility according to standard protocols. Incubation with biotinylated secondary antibody against rabbit (Vector Laboratories, Burlingame, CA) was followed by the ABC reagent (Vector Laboratories). 3,3′-Diaminobenzidine (Dako) was used for detection. Nuclei were counterstained with hematoxylin Harris (Leica, Wetzlar, Germany).

Mice and aGVHD experiments

Female C57BL/6 (B6) (H2^b), LP/J (H2^b), 129 (H2^b), and B6D2F1 (BDF) (H2$^{b/d}$) mice (10–12 weeks old) were purchased from Charles River Laboratories (Sulzfeld, Germany), BALB/c (H2^d) mice (10–12 weeks old) were purchased from Janvier (St. Berthevin Cedex, France) and housed in the Charité University Hospital Animal Facility. aGVHD models were used as described previously.[2-4] For chemotherapy based models, 7 days before bone marrow transplantation (BMT), female B6 or BDF mice received 20mg/kg/day busulfan (Sigma Aldrich, USA) i.p. on 5 consecutive days. Additionally, 5 days before BMT, 100mg/kg/day cyclophosphamide

monohydrate (Sigma Aldrich, USA) was applied by i.p. injection on 3 consecutive days. B6 mice received 1×10^7 BM and 2×10^7 T-cells from LP/J or 129 donors, BDF mice received 1×10^7 BM and 5×10^6 T-cells. For the radiation based model, female BALB/c mice received 800 centigray (cGy) total body irradiation from a ^{137}Cs source (GSR D1, Gamma Service Medical, Germany) with a maximum of 0.85cGy per min as a split dose and received $0,5 \times 10^7$ BM and 1×10^6 T-cells from B6 donor mice on the same day. Control groups (no GVHD) were transplanted with the same BM cell numbers and T-cell numbers from syngeneic donors. The Regional Ethics Committee for Animal Research approved all animal experiments. To mimic SR-aGVHD, we used the chemotherapy based murine models 129→B6 MHC-matched and B6→B6D2F1 (haploidentical) and the radiation based murine model BALB/c→B6 major MHC-mismatch with conditioning and cell dosages analogue to the models described above. Recipient mice were treated intraperitoneal with 0.5mg/kg/d dexamethasone beginning at day+4 after allo-HSCT (Merck, Darmstadt, Germany).[5, 6] We used dexamethasone because of its longer lasting effects as compared with methyl-prednisolone or prednisolone enabling once daily dosing in the murine models. The rationale for starting at day+4 is that during this time leukocytes start to infiltrate target organs during aGVHD.[3, 4, 7] Clinical scores, weight loss and survival in the B6-BDF SR-aGVHD model are given in supplementary figure 1.

Conventional transmission electron microscopy (TEM)

aGVHD was induced in the B6→BDF model and organs were harvested, fixed and embedded with propylene oxide (SERVA, Heidelberg, Germany) and epoxy resin (SERVA). Ultra-thin sections (70nm) were prepared with an Ultracut S ultramicrotome (Leica). Staining was performed with uranyl acetate and lead citrate according to Reynolds. Microscopy was performed with an EM 906 electron microscope (ZEISS, Oberkochen, Germany).

Histology of murine tissues

Tissue samples were cryoembedded and scored as previously described.[1] The following antibodies were used: αSMA, Sigma-Aldrich, 1A4; ZO-1, Thermo Scientific, polyclonal; VE-cadherin, R&D, polyclonal; CD31, BD, 2H8; Lyve1, R&D, 223322; CD4, BD, H129.19. Microscopy was performed with BA410 epifluorescence microscope and marker$^+$ area to total area was quantified by Fiji Software.

Evans blue assay

For assessment of endothelial leakage, Evans blue assay was performed as described in detail elsewhere.[8] Briefly, mice from B6→BDF aGVHD model received an i.v. injection of a sterile 1% (w/v) Evans blue (Sigma-Aldrich) solution. Organs were harvested 30 minutes after injection, weighted and placed in tubes containing formalin solution (Roth, Germany). Evans blue in the supernatant was determined at a wavelength of 610nm with a Benchmark plus microplate spectrometer system (BioRad, USA). The extravasation of Evans blue from the blood vessels was calculated taking into account the organ weight in mg.

Immunolabeling against VE-cadherin for light sheet fluorescence microscopy

25µg/mouse anti-VE-cadherin antibody (Thermo Scientific, eBioBV13-eFluor660) was i.v. injected in mice from B6→BDF aGVHD model. Mice were sacrificed and perfused with PBS followed by 4% paraformaldehyde in PBS. Sample preparation and imaging of whole organs were performed by light sheet fluorescence microscopy as previously described.[9] Analysis of vasculature and its segmentation were performed using Imaris 8.1 software (Bitplane, Concord, MA). Branch level was determined by branching point and diameter changes of the vasculature.[10]

Cell line and *in vitro* assays

Mouse cardiac endothelial cells (MCECs) were cultured in supplemented DMEM medium. 100nm etoposide (eto, Sigma-Aldrich) was added to induce apoptosis. The MTT assay (Sigma-Aldrich) was performed according to the manufactures protocol.

Flow cytometry

Cells were washed twice and stained for 20 minutes at 4°C in PBS/0.5 mM EDTA/0.5% BSA with the following rat mAbs from BD Biosciences:

anti-CD11b (M1/70-APC-Cy7), anti-CD31 (MEC13.3-APC and PE), anti-CD45 (30F11-PerCP-Cy5.5 and FITC), anti-CD80 (16-10AA-PE) anti-CD86 (GL1-APC) anti-Ter119 (Ter119-PE-Cy7), anti-H2^b (MHCI, AF6-88.5-FITC), anti-MHCII (OX6-PerCp). Samples were analyzed by BD FACSCanto II (BD Biosciences) and FlowJo 7.6.5 Software (TreeStar Inc, Ashland, OR).

Hepatic endothelial cell isolation

Single cell suspensions were generated via digestion with 2mg/ml collagenase D and 5µl deoxyribonuclease. Hepatic endothelial cell fraction was enriched by gradient centrifugation using 30% histodenz (Sigma Aldrich). For gene expression analysis, the obtained single cell suspension was further enriched for endothelial cells (CD11b$^-$, CD45$^{dim/-}$, CD31$^+$) by flow cytometry using a Bio-Rad S3 cell Sorter. Endothelial cell purity was determined via flow cytometry analysis of ICAM1$^+$ and CD31$^+$ cells.

Statistics

Survival data were analyzed using the Kaplan–Meier method and compared with the Mantel–Cox log-rank test. For statistical analysis of all other data, Student's *t*-test was used, unless indicated otherwise. Values are presented as mean ± SEM. Values of $p \leq 0.05$ were considered as statistically significant. All statistical analyses were performed using GraphPad Prism software (GraphPad Software Inc., La Jolla, CA).

Methods used for supplementary data

In Vivo T-Cell Proliferation Assay

BALB/c recipients were conditioned with 800cGY TBI. CD3$^+$ lymphocytes were isolated from spleens of B6 donors and enriched by Pan T-Cell isolation kit (Milteny Biotec, Bergisch Gladbach, Germany). CFSE-loaded CD3$^+$ cells were injected i.v. into the tail vein. Ninety-six hours later, mice were sacrificed, spleens, blood and lymph nodes were taken, and cells were isolated.

Microarray analysis

Total RNA from hepatic endothelial cells harvested at day+15 after allo-HSCT was isolated with the mirVana^{TM} miRNA Isolation Kit (Life Technologies, USA) and subjected to microarray analysis (GeneChip® Mouse Gene 2.0 ST Array, Affymetrix, USA) at Max Delbrück Center core facility for Genomics. The raw data were normalized with Expression Console Software and analyzed with Transcriptome Analysis Console (TAC) Software (Affymetrix, USA) using the following parameters: Fold change (linear) < -2 or > 2, ANOVA P-value (Condition pair) < 0.05 (multiple testing correction with Bonferroni).

Vessel wire myography

Vessel wire myograph is a well-established method to test isometric transversal tension of isolated vessels in response to physiological and pathopysiological stimuli. Monitoring of the ex vivo vessel tension to the different stimuli gives information of endothelial and pericyte function, controlling the vessel tonus. In human GVHD pathogenesis, physiological information is hard to obtain: the data are compromised by prophylactic treatment with drugs such as glucocorticoids and calcineurin inhibitors. Both are described to lead to increased blood pressure and alteration of physiologic functions. Contraction of isolated mesenteric arteries was measured using a conventional small vessel wire DMT 610M myograph. Mesenteric arteries were isolated, dissected, mounted on two stainless steel wires in a 2 ml organ bath filled with PSS, as described previously.[11] The software Chart5 (AD Instruments Ltd.) was used for data acquisition and display. Vessel constriction was provoked by

noradrenaline (NA) and phenylephrine (Phe) at the concentrations indicated. Finally, acetylcholine (ACh) was used to investigate relaxation.[11, 12]

References

1.   Lerner KG, Kao GF, Storb R, Buckner CD, Clift RA, Thomas ED. Histopathology of graft-vs.-host reaction (GvHR) in human recipients of marrow from HL-A-matched sibling donors. *Transplant Proc* 1974; **6**(4)**:** 367-371. e-pub ahead of print 1974/12/01;

2.   Mertlitz S, Shi Y, Kalupa M, Grotzinger C, Mengwasser J, Riesner K *et al.* Lymphangiogenesis is a feature of acute GVHD, and VEGFR-3 inhibition protects against experimental GVHD. *Blood* 2017; **129**(13)**:** 1865-1875. e-pub ahead of print 2017/01/18; doi: 10.1182/blood-2016-08-734210

3.   Riesner K, Kalupa M, Shi Y, Elezkurtaj S, Penack O. A preclinical acute GVHD mouse model based on chemotherapy conditioning and MHC-matched transplantation. *Bone marrow transplantation* 2016; **51**(3)**:** 410-417. e-pub ahead of print 2015/11/26; doi: 10.1038/bmt.2015.279

4.   Riesner K, Shi Y, Jacobi A, Krater M, Kalupa M, McGearey A *et al.* Initiation of acute graft-versus-host disease by angiogenesis. *Blood* 2017; **129**(14)**:** 2021-2032. e-pub ahead of print 2017/01/18; doi: 10.1182/blood-2016-08-736314

5.   Bouazzaoui A, Spacenko E, Mueller G, Huber E, Schubert T, Holler E *et al.* Steroid treatment alters adhesion molecule and chemokine expression in experimental acute graft-vs.-host disease of the intestinal tract. *Experimental hematology* 2011; **39**(2)**:** 238-249 e231. e-pub ahead of print 2010/11/27; doi: 10.1016/j.exphem.2010.11.006

6.   Toubai T, Rossi C, Tawara I, Liu C, Zajac C, Oravecz-Wilson K *et al.* Murine Models of Steroid Refractory Graft-versus-Host Disease. *Scientific reports* 2018; **8**(1)**:** 12475. doi: 10.1038/s41598-018-30814-x

7.   Beilhack A, Schulz S, Baker J, Beilhack GF, Wieland CB, Herman EI *et al.* In vivo analyses of early events in acute graft-versus-host disease reveal sequential infiltration of T-cell subsets. *Blood* 2005; **106**(3)**:** 1113-1122. e-pub ahead of print 2005/04/28; doi: 10.1182/blood-2005-02-0509

8.   Radu M, Chernoff J. An in vivo assay to test blood vessel permeability. *Journal of visualized experiments : JoVE* 2013; (73)**:** e50062. e-pub ahead of print 2013/03/26; doi: 10.3791/50062

9.   Brede C, Friedrich M, Jordan-Garrote AL, Riedel SS, Bauerlein CA, Heinze KG *et al.* Mapping immune processes in intact tissues at cellular resolution. *The Journal of clinical investigation* 2012; **122**(12)**:** 4439-4446. e-pub ahead of print 2012/11/13; doi: 10.1172/jci65100

10. Wertheimer T, Velardi E, Tsai J, Cooper K, Xiao S, Kloss CC *et al.* Production of BMP4 by endothelial cells is crucial for endogenous thymic regeneration. *Sci Immunol* 2018; **3**(19). doi: 10.1126/sciimmunol.aal2736

11. Bridges LE, Williams CL, Pointer MA, Awumey EM. Mesenteric Artery Contraction and Relaxation Studies Using Automated Wire Myography. *Journal of visualized experiments : JoVE* 2011; (55). doi: 10.3791/3119

12. Dietrich A, Mederos YSM, Gollasch M, Gross V, Storch U, Dubrovska G *et al.* Increased vascular smooth muscle contractility in TRPC6-/- mice. *Molecular and cellular biology* 2005; **25**(16)**:** 6980-6989. e-pub ahead of print 2005/08/02; doi: 10.1128/mcb.25.16.6980-6989.2005

Supplementary figures
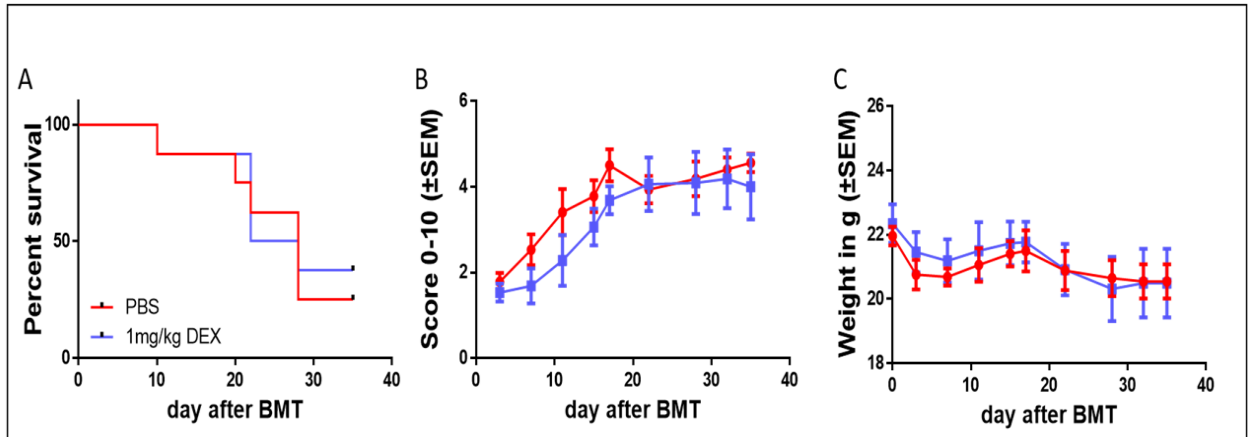
**Supplementary Figure 1) Steroid treatment in an experimentally aGVHD model.** Shown is the clinical data of the model presented in Figure 5 of the manuscript. We treated allo-HSCT recipients with aGVHD either with PBS (ctr) or Dexamethasone (Dex) starting at day +4 in the chemotherapy based B6→BDF model. Shown are A) survival, B) clinical aGVHD scores of the surviving animals and C) weight of the surviving animals in g over time.
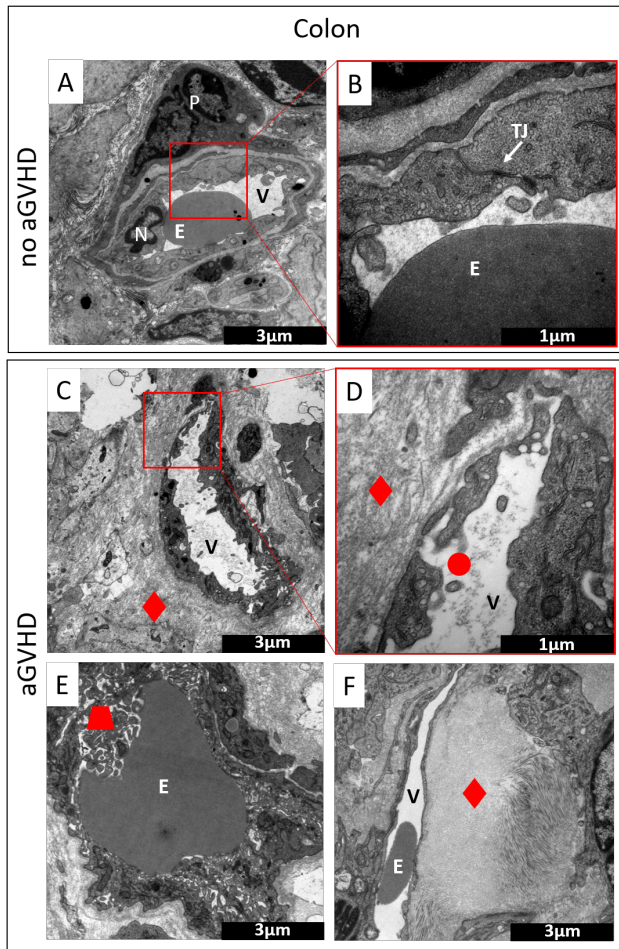
Supplementary Figure 2) Visualization of GVHD-associated ultrastructural changes in the colon by transmission electron microscopy. Shown are typical pictures of sections from colon taken at day+15 after experimental HSCT in the chemotherapy based B6→BDF model. Control groups (no GVHD) were transplanted with the same BM cell numbers and T-cell numbers from syngeneic donors. **G-H)** Colonic mucosa endothelium after allo-HSCT without aGVHD. **G)** Unaltered endothelial monolayer with a prominent endothelial-endothelial cell contact. The vessel is surrounded by a pericyte. **H)** Higher magnification of an intact endothelial-endothelial cell contact. **I-L)** Colonic mucosa endothelium during aGVHD. **I)** Ruffled, activated endothelium with many vesicles in the endothelial cytoplasm and reduced thickness of the endothelial monolayer. The vessel is surrounded by perivascular fibrinogen deposits marked by a red rhombus. **J)** Higher magnification of the endothelial monolayer, showing vesicles and irregular thickness of the endothelium marked by a red circle. Perivascular fibrinogen deposits are marked by a red rhombus. **K)** Vessel in mucosa filled with an erythrocyte; the endothelial monolayer is strongly convolved, marked with a red trapezoid. **L)** Vessel in colonic mucosa with prominent perivascular fibrinogen accumulation marked by a red rhombus. (V, vessel lumen; E, erythrocyte; P, pericyte; N, nucleus; TJ, tight

junction; red rhombus, perivascular fibrinogen deposits; red circle, irregular, activated endothelium; red trapezoid, endothelial convolution)
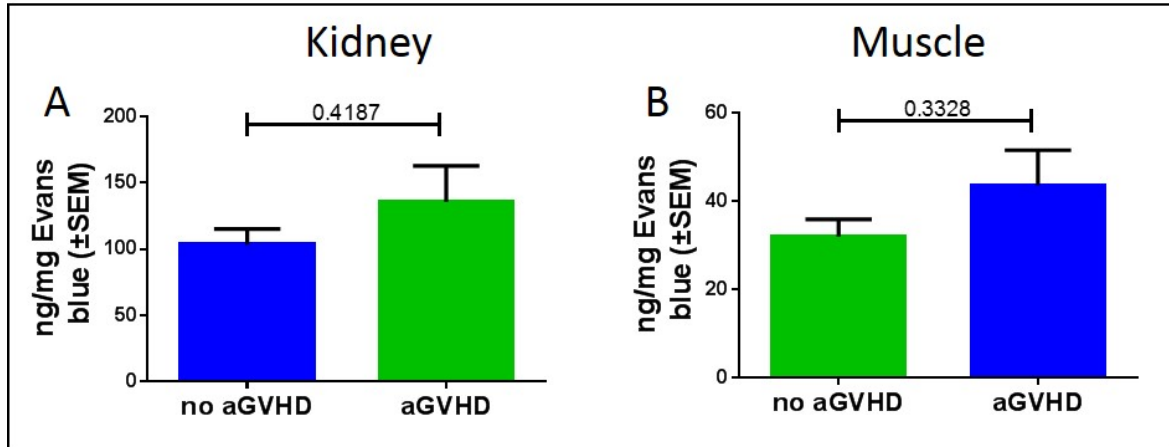
Supplementary Figure 3) Assessment of endothelial leakage in non-target organs of aGVHD. A-B) Measurement of Evans blue extravasation at day+15 after experimental HSCT in the chemotherapy based B6→BDF model. Control groups (no aGVHD) were transplanted with the same BM cell numbers and T-cell numbers from syngeneic donors. Quantification of Evans blue extravasation in ng Evans blue per mg **A)** kidney and **B)** skeletal muscle of HSCT recipients with aGVHD versus without aGVHD. Significance was tested by student's *t*-test (n=5-6 animals per group). Error bars indicate mean ± standard error of the mean (SEM).
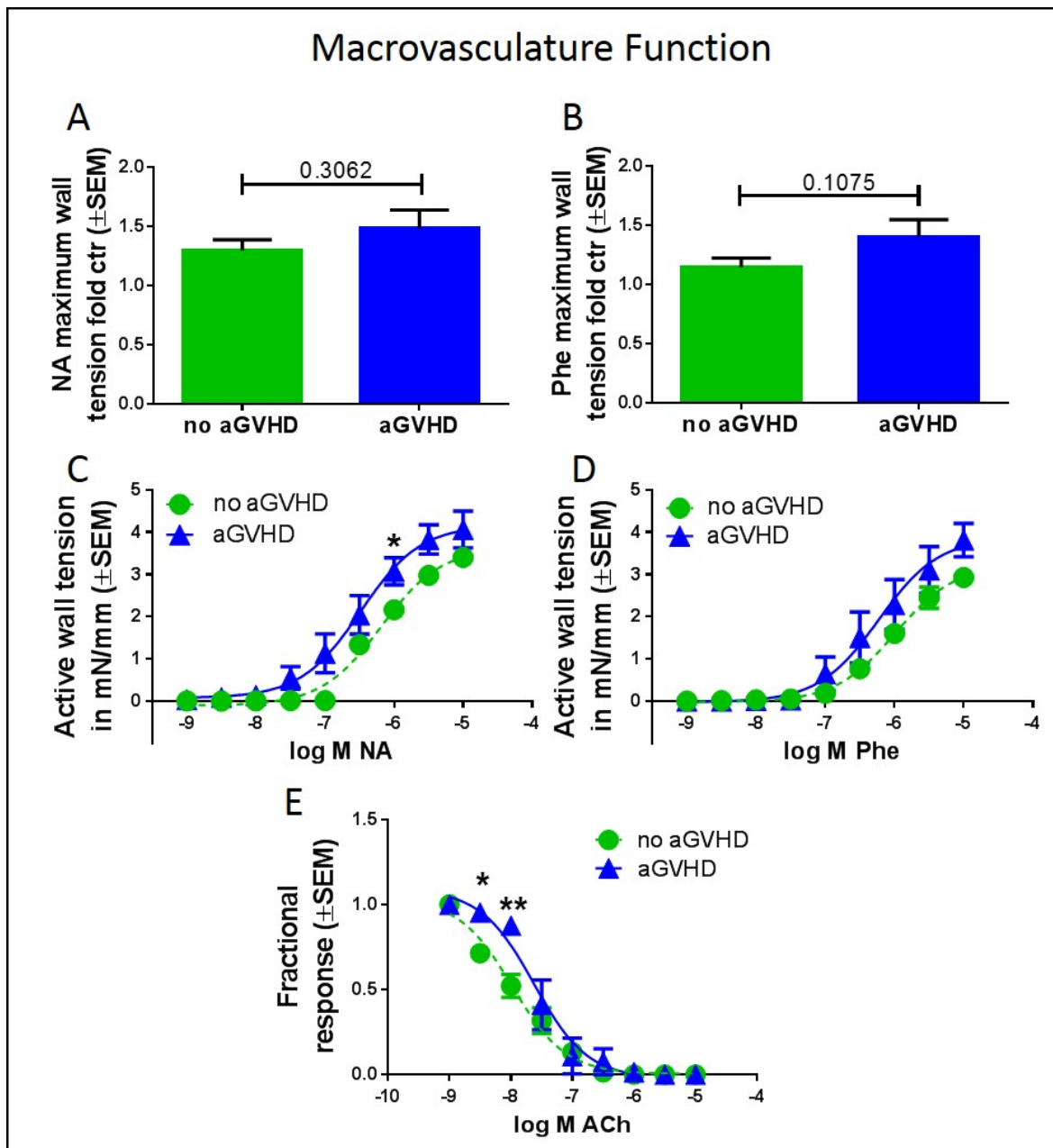
Supplementary Figure 4) Physiological functions of mesenteric arteries. A-B) Maximum contraction of mesenteric arteries upon different stimuli at day+29 after experimental allo-HSCT in the chemotherapy based LP/J→B6 model. Control groups (no aGVHD) were transplanted with the same BM cell numbers and T-cell numbers from syngeneic donors. Maximum contraction of mesenteric arteries in response to **A)** noradrenaline (NA) and **B)** phenylephrine (Phe) from HSCT recipients with aGVHD versus no aGVHD. **C-D)** Partial contraction of mesenteric arteries upon increasing concentrations of **C)** NA and **D)** increasing concentrations of Phe. **E)** Partial relaxation of mesenteric arteries induced by acetylcholine (ACh) after maximum contraction with potassium. Significance was tested by student's *t*-test (*$P < .05$; **$P < .01$; n=6 to 8 mesenteric arteries from 3 to 4 animals). Error bars indicate mean ± standard error of the mean (SEM).
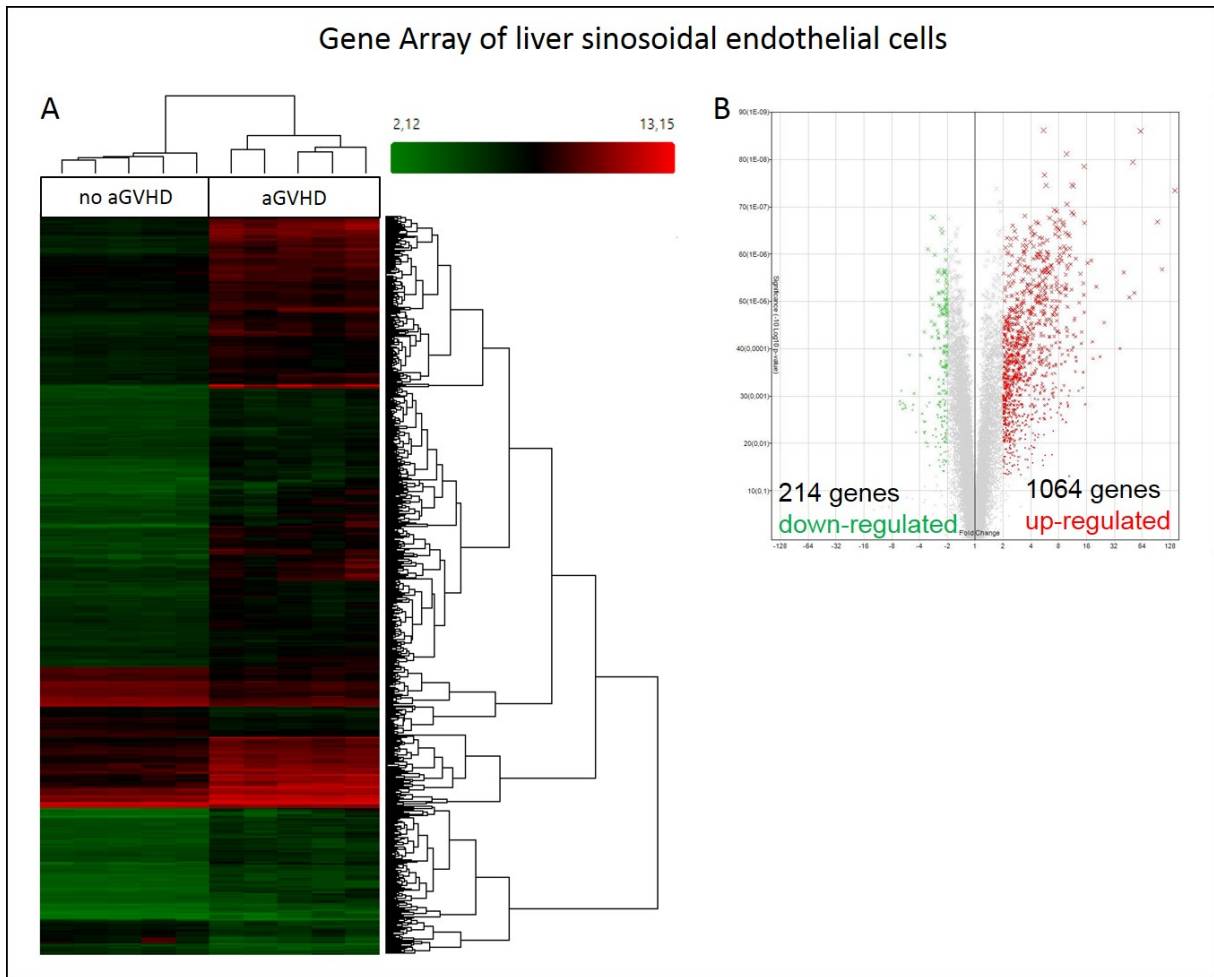
Supplementary Figure 5) Microarray analysis of sorted hepatic endothelial cells after allo-HSCT. A-B) Gene array from isolated hepatic endothelial cells from HSCT recipients at day+15 in the chemotherapy based LP/J→B6 model. Control groups (no aGVHD) were transplanted with the same BM cell numbers and T-cell numbers from syngeneic donors. Gene expression changes between the aGVHD group and no aGVHD group were analyzed. **A)** Hierarchical clustering of microarray data. Green and red represent low and high levels of gene expression. **B)** Volcano plot showing the expression of total genes; red and green crosses represent 1064 up-regulated and 214 down-regulated genes, respectively. (n= 5 animals per group).
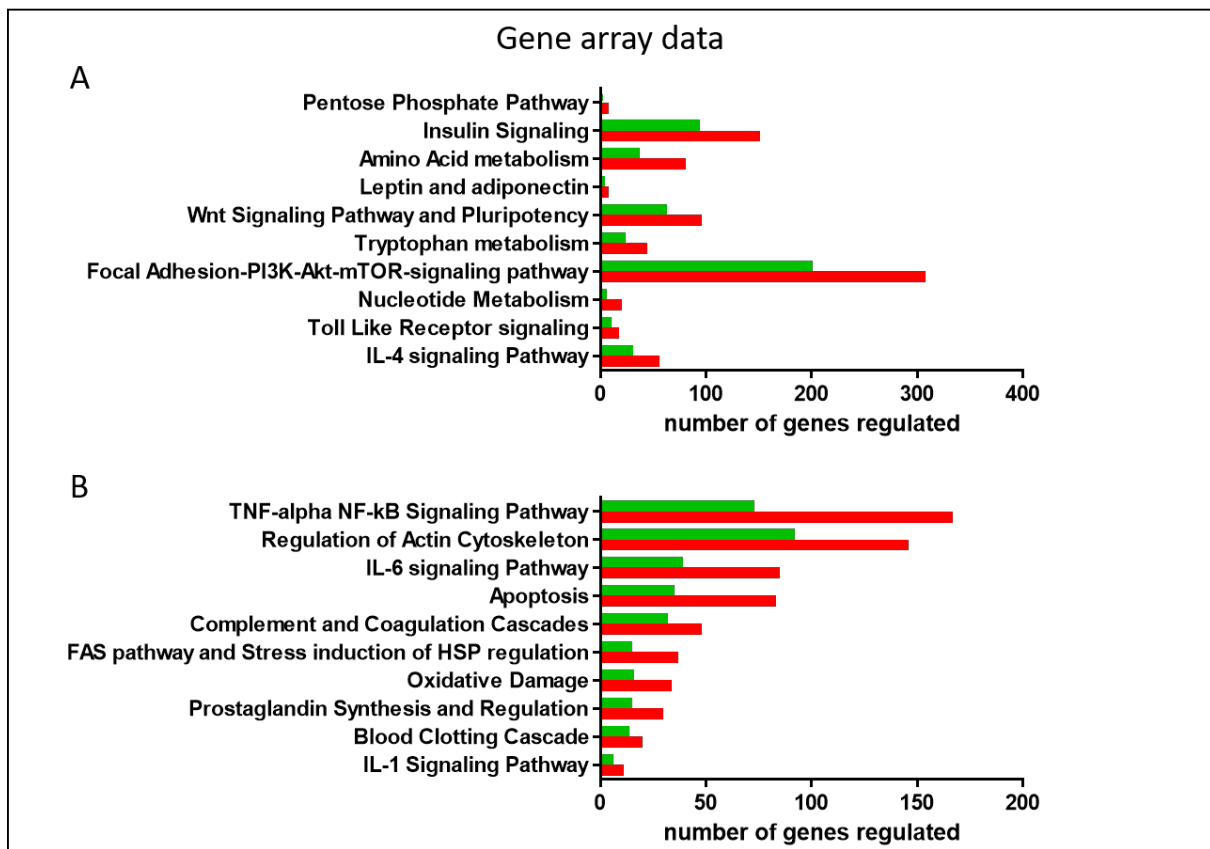
Supplementary Figure 6) Pathways identified by microarray analysis of sorted hepatic endothelial cells during aGVHD. Gene array from isolated hepatic endothelial cells at day+15 after experimental HSCT in the chemotherapy based LP/J→B6 model. Control groups (no aGVHD) were transplanted with the same BM cell numbers and T-cell numbers from syngeneic donors. Gene expression changes between the aGVHD group and no aGVHD group were analyzed. **A)** Selected pathways are grouped according to biologic relevance. The red bars show the number of up-regulated genes during aGVHD. Accordingly, numbers of down-regulated genes during aGVHD are displayed as green bar. **B)** Damage associated pathways identified by microarray analysis of sorted hepatic endothelial cells during aGVHD. Selected pathways are sorted after relevance. In the first (gray) column pathways are listed. The red bars show the number of up-regulated genes during aGVHD. Accordingly, numbers of down-regulated genes during aGVHD are displayed as green bar.
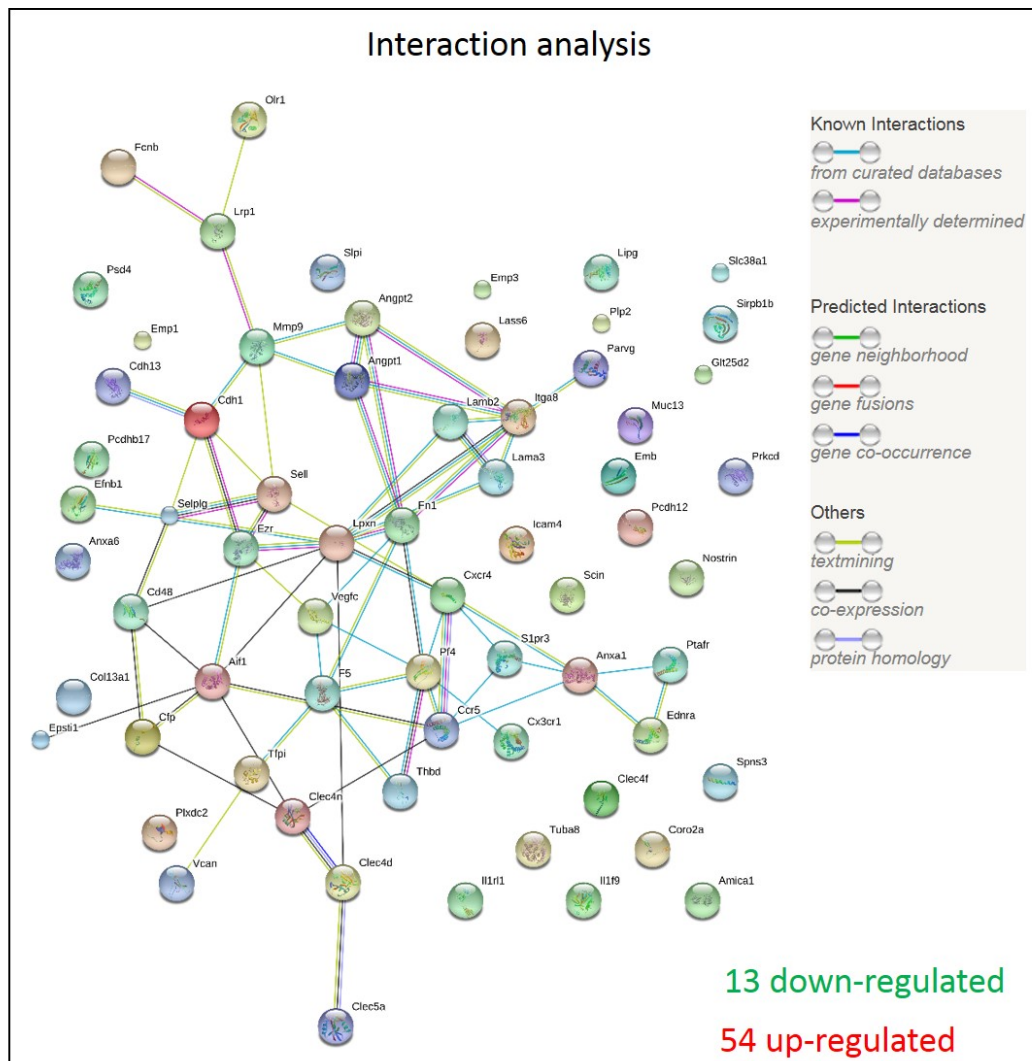
Supplementary Figure 7) Interactive network of regulated genes. Gene array from isolated hepatic endothelial cells from HSCT recipients at day+15 in the chemotherapy based LP/J→B6 model. Control groups (no aGVHD) were transplanted with the same BM cell numbers and T-cell numbers from syngeneic donors. Gene expression changes between the aGVHD group and no aGVHD group were analyzed. Shown is the network analysis of selected, endothelium specific genes in hepatic endothelial cells. Several interaction partners on protein levels among the regulated genes were identified. Analysis was performed with String database (https://string-db.org/).
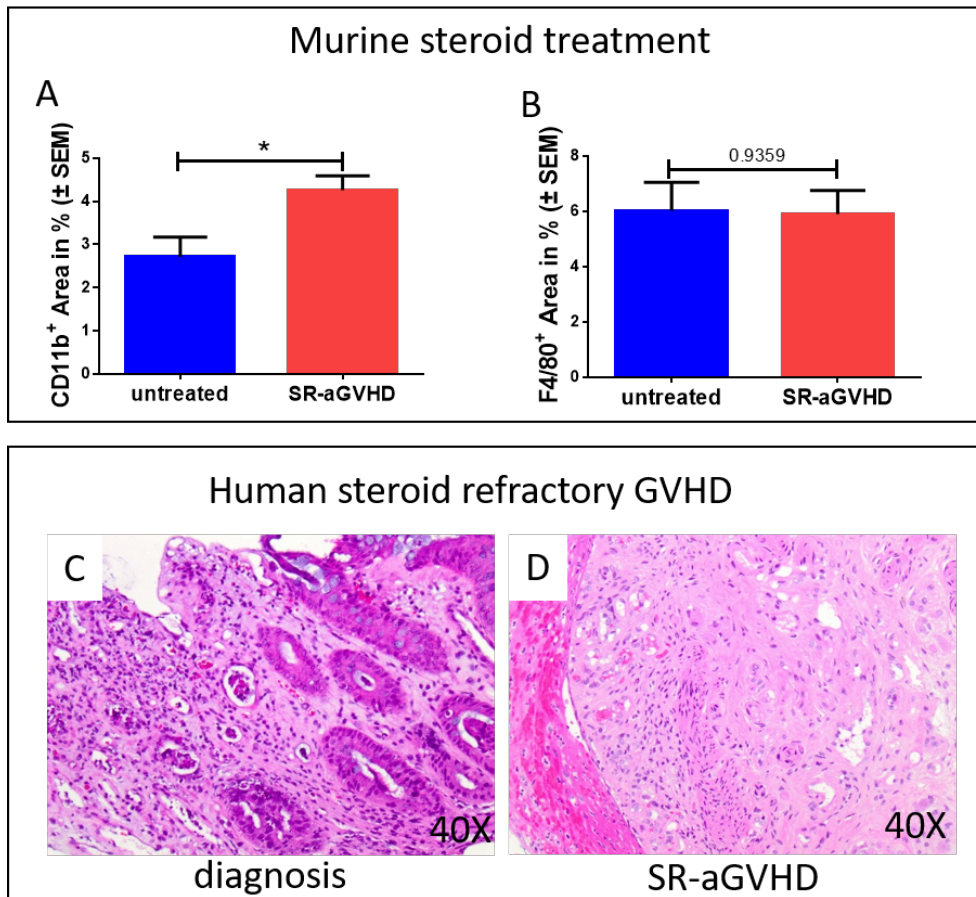
Supplementary Figure 8) Immune cell infiltration and endothelial damage in an experimentally murine SR-aGVHD model and in an independent human SR-aGVHD cohort. A-B) Immune cell infiltration in colon samples at day+15 after experimental allo-HSCT in the chemotherapy based B6→BDF model. Quantification of CD11b$^+$ area in colonic mucosa of control PBS treated (untreated) aGVHD versus Dexamethasone treated aGVHD (SR-aGVHD, 0.5mg/kg/day Dexamethasone starting at day+4) **B)** Quantification of F4/80$^+$ area in colonic mucosa of untreated aGVHD versus SR-aGVHD. Significance was tested by student's *t*-test (****P* < .001; n=5 animals per group). Error bars indicate mean ± standard error of the mean (SEM). **C-D)** Human colon biopsies stained for HE during the course of SR-aGVHD. **A)** Colon biopsy with inflammatory infiltration and apoptotic crypt cells at diagnosis of aGVHD. **B)** Colon biopsy of the same patient with progressive SR-aGVHD after 89 days of Prednisolone treatment. Loss of colonic mucosa structure and low degree of inflammatory infiltrates.
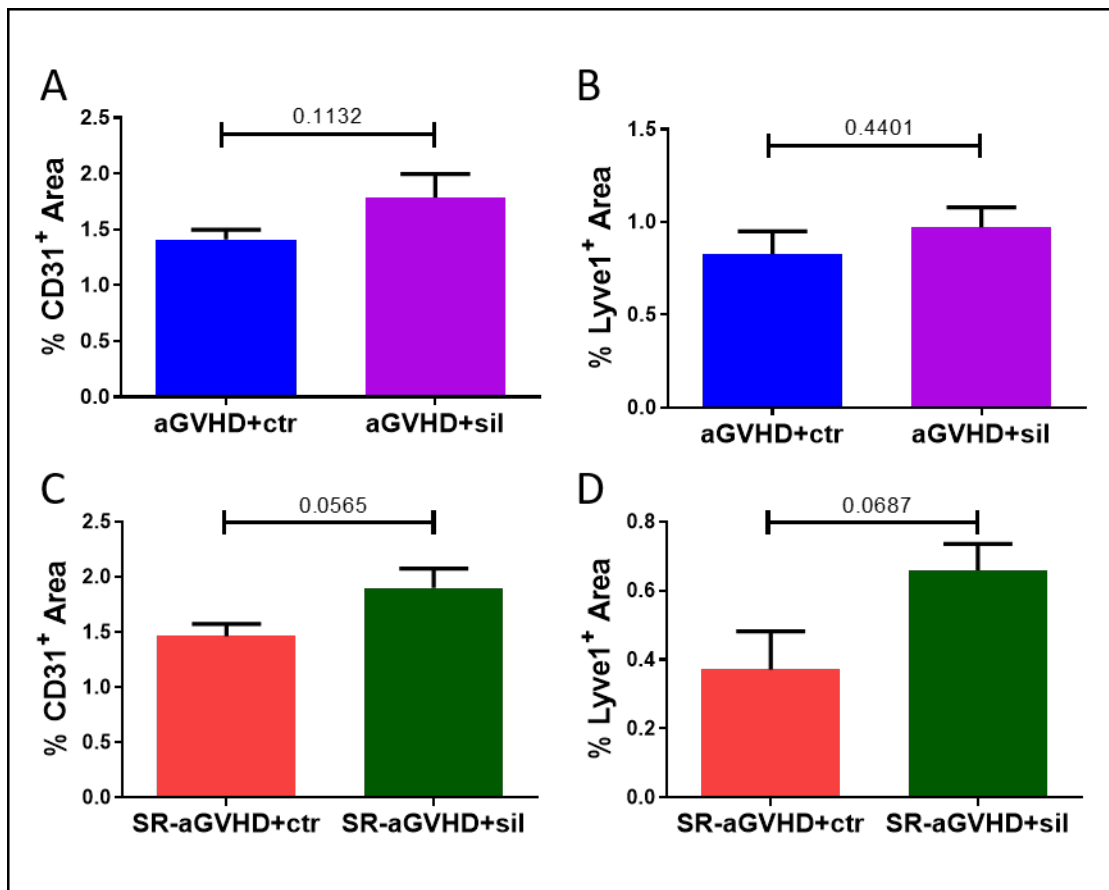
Supplementary Figure 9) *In vivo* treatment of aGVHD and SR-aGVHD with sildenafil. **A -**
B) Treatment of aGVHD with 10mg/kg/d sildenafil at day+15 after experimental allo-HSCT in
the radiation based B6→BALB/c model. **A)** Histological analysis of vascular density with
endothelial cell marker CD31 and **B)** histological analysis of lymphatic vascular density with
lymphatic endothelial marker Lyve1 in colon of sildenafil (aGVHD+sil) versus control
substance (aGVHD+ctr) treated allo-HSCT recipients at day+15. **C-D)** Treatment with
10mg/kg/d sildenafil in a murine model of SR-aGVHD at day+15 after experimental allo-
HSCT in the radiation based B6→BALB/c model. **B)** Histological analysis of angiogenesis
with endothelial cell marker CD31 and **D)** histological analysis of lymphangiogenesis with
lymphatic marker Lyve1 in colon in sildenafil (SR-aGVHD+sil) versus control substance (SR-
aGVHD+ctr) treated allo-HSCT recipients at day+15.
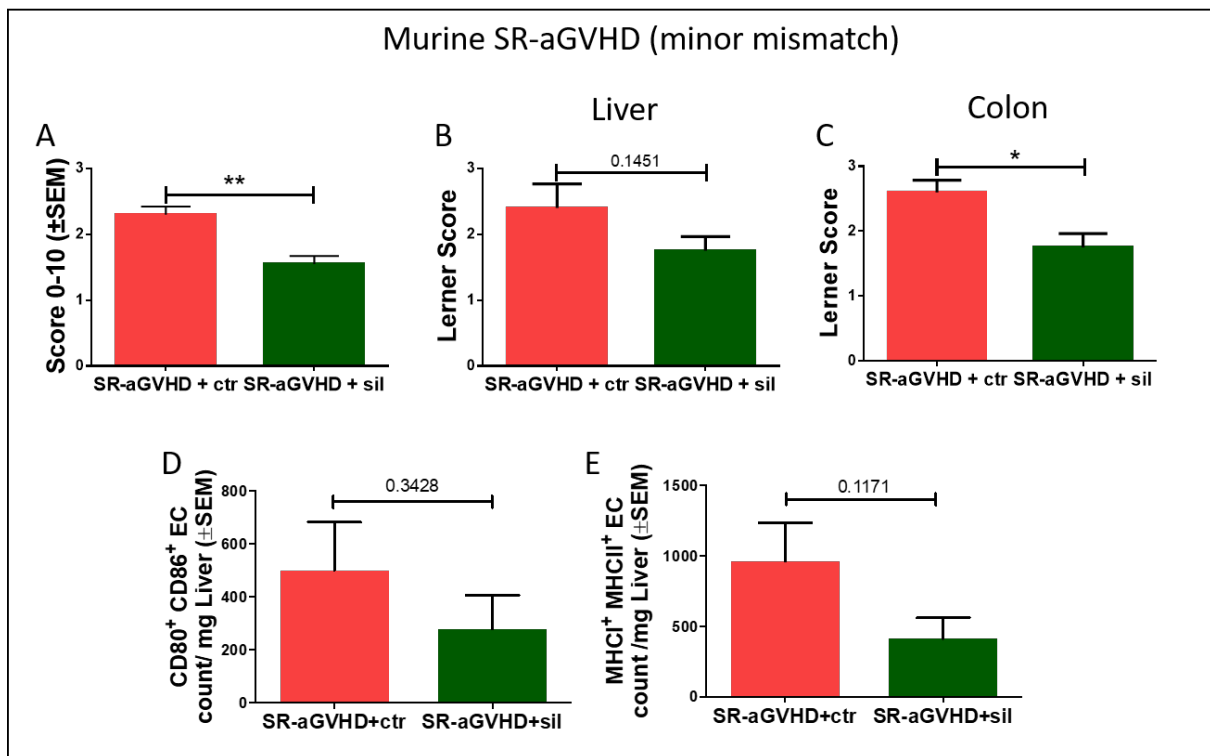
Supplementary Figure 10) *In vivo* **treatment of SR-aGVHD with sildenafil. A-E)** Treatment of SR-aGVHD with 10mg/kg/d sildenafil after experimental allo-HSCT at day+15 in the chemotherapy based 129→B6 model. **A)** Clinical Score of Sildenafil (SR-aGVHD+sil) versus control substance treated (SR-aGVHD+ctr) SR-aGVHD. Histopathological assessment of aGVHD severity in **B)** liver and **C)** colon in SR-aGVHD+sil and SR-aGVHD+ctr at day+15 after allo-HSCT. Flow cytometry quantification of **D)** MHCI and MHCII expression and **E)** CD80 and CD86 expression of isolated liver sinusoidal endothelial cells of SR-aGVHD+sil and SR-aGVHD+ctr at day+15 after allo-HSCT. Significance was tested by student's *t*-test (*$P < .05$; **$P < .01$; n=5-6 animals per group). Error bars indicate mean ± standard error of the mean (SEM).
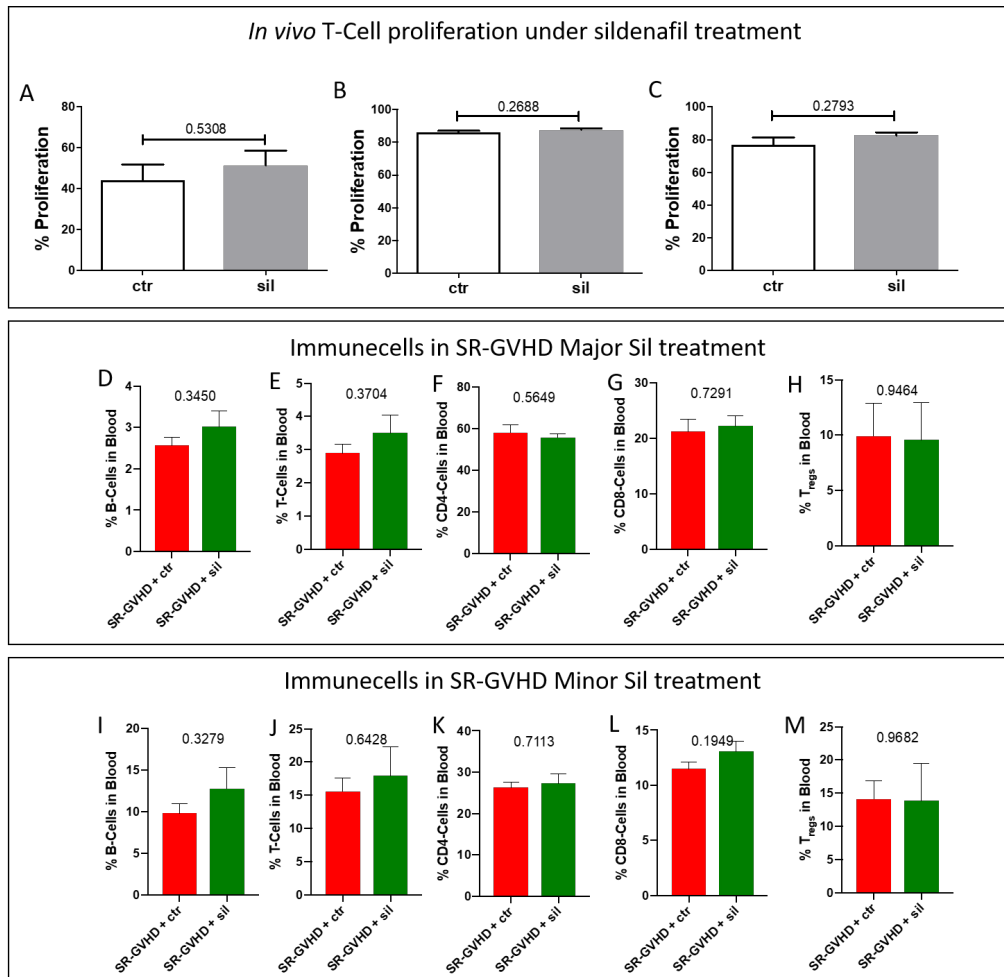
Supplementary Figure 11) In vivo proliferation of T-cells under Sildenafil treatment. A-D) CFSE labeled T-cells from B6 mice were transferred in radiated BALB/c mice treated with PBS/DMSO (ctr) or 10mg/kg/d Sildenafil (sil) for 4 days. Afterwards T-cells from recipients were isolated from **A)** spleen, **B)** peripheral blood and **C)** lymph nodes and analyzed by flow cytometry. CFSE$^-$CD3$^+$ events were defined as proliferated T-cells. Significance was tested by student's *t*-test (n=4 animals per group). Error bars indicate mean ± standard error of the mean (SEM). Immune cells in blood of SR-aGVHD and SR-aGVHD animals treated with 10mg/kg/d Sildenafil at d+15 after allo-HSCT in **D-H)** the radiation based BALB/c→B6 and the **(I-M)** chemotherapy based 129→B6 model. Flow cytometric quantification of **D)** B-cell Marker B220, **E)** T-cell receptor CD3, **F)** CD4 and **G)** CD8 T-cell co-receptors and **H)** CD4+ CD25^{high} FoxP3$^+$ regulatory T-cells. Flow cytometric quantification of **I)** B-cell Marker B220, **J)** T-cell receptor CD3, **K)** CD4 and **L)** CD8 T-cell co-receptors and **M)** CD4+ CD25^{high} FoxP3$^+$ regulatory T-cells. Significance was tested by student's *t*-test (n=5-6 animals per group). Error bars indicate mean ± standard error of the mean (SEM).

Supplementary Table 1. Patient Characteristics Figure 1c. Endothelial apoptosis in duodenal biopsies of patients after alloSCT without GVHD vs. GVHD.

	No GVHD									GVHD										
Patient Nr.	1	2	3	4	5	6	7	8	9	10	11	12	13	14	15	16	17	18	19	20
Age at alloSCT	57	24	52	31	64	34	55	44	59	50	49	42	64	47	19	52	56	26	25	52
Recipient sex	m	m	f	f	f	m	f	m	m	m	m	f	f	f	m	m	m	f	m	f	f
Donor sex	m	m	f	f	m	m	m	m	m	m	m	f	f	m	m	m	f	m	f	f
Donor RD			x							x	x									
MUD	x	x		x	x	x	x	x				x		x	x			x	x	x
MMUD									9/10				9/10			9/10	9/10			
Disease AML, MDS	AML				AML				AML			MDS	AML	AML		AML	MDS			MDS
ALL				ALL			ALL								ALL			ALL		
Lymphoma										DLBCL										
MPS						CML					CML									
Multiple Myeloma			MM					MM												
Non-malignant		AA																	AA	
Stem cell source Peripheral stem cells	x	x	x	x	x	x	x	x	x	x	x	x	x	x	x	x	x	x		x
Bone marrow stem cells																			x	
Conditioning Reduced intensity (RIC)	Bu/Flu	Cy	Flu/Mel		Bu/Flu	Bu/Flu	TBI/Flu	Treo/Flu	TBI/Flu				Bu/Flu	Treo/Flu		Treo/Cy	Bu/Flu		Cy	Flu/Bu
Myeloablative (MAC)				Cy/TBI						Cy/TBI	Cy/TBI	Cy/TBI			Cy/TBI			Cy/TBI		
Maximum grade intestinal aGVHD	0	0	0	0	0	0	0	0	0	3	3	4	3	3	3	3	3	4	4	4
Onset of acute GVHD day post alloSCT	N/A	N/A	N/A	N/A	N/A	N/A	N/A	N/A	N/A	+45	+55	+144	+66	+88	+32	+271 Post DLI	+20	+34	+56	+62
Biopsy taken																				

day post alloSCT	+134	+98	+48	+23	+72	+21	+107	+92	+43	+47	+58	+149	+74	+92	+34	+275	+22	+39	+59	+65
GVHD prophylaxis medication	CSA/MMF	CSA/MMF	CSA/MTX	CSA/MTX	CSA/MMF	CSA/MMF	CSA/MTX	CSA/MTX	CSA/MTX	CSA/MTX	CSA/MTX	CSA/MTX	CSA/MMF	CSA/MTX	CSA/MTX	CSA/MTX	CSA/MMF	CSA/MTX	CSA/MTX	CSA/MMF
Microangiopathy (TMA)	No	No	No	No	No	No	No	No	No	No	No	No	No	No	No	No	No	No	No	No

Abbreviations: RD - related donor, MUD – matched unrelated donor, MMUD – mismatched unrelated donor, AML – acute myeloid leukemia, ALL – acute lymphoid leukemia, MPS – myeloproliferative syndrome, AA – aplastic anemia, CSA – Cyclosporine A, MMF – Mycophenolate mofetil, MTX – Methotrexate

Supplementary Table 2. Patient Characteristics Figure 1d. Endothelial apoptosis in colon biopsies of patients after alloSCT without GVHD vs. GVHD.

	No GVHD							GVHD							
Patient Nr.	1	2	3	4	5	6	7	8	9	10	11	12	13	14	15
Age at alloSCT	63	57	55	58	21	46	60	52	47	45	48	61	48	31	52
Recipient sex	f	m	m	f	m	m	f	m	m	f	f	m	m	m	f
Donor sex	f	m	m	m	m	m	f	m	m	f	m	f	m	m	f
Donor RD			x												
MUD	x	x		x	x		x		x	x	x			x	x
MMUD						MM UD		MM UD					MM UD		
Haplo															
Disease AML, MDS	MDS	AML	AML	AML		AML	AML		AML	AML	AML				MDS
ALL					ALL									ALL	
Lymphoma												HCL			
MPS								PV/ OMF							
Multiple Myeloma													MM		
Non-malignant															
Stem cell source Peripheral blood	x	x	x	x	x	x	x	x	x	x	x	x	x	X 2nd	x
Bone marrow															
Condition-ing RIC	Bu/Flu	Bu/Flu	Bu/Flu	Bu/Flu		Flam sa	Bu/Flu	Bu/Flu	Bu/Flu		Bu/Flu	Bu/Flu	Treo/Flu	Flu	Flu/ Bu
MAC, Aplasia conditioning					Cy/TBI					Cy/TBI					
Maximum grade intestinal aGVHD	0	0	0	0	0	0	0	4	3	3	3	3	3	4	3
Onset of acute GVHD day post alloSCT	N/A	N/A	N/A	N/A	N/A	N/A	N/A	+89	+61	+110	+41	+95	+84	+121	+62
Biopsy taken day post alloSCT	+61	+134	+70	+46	+24	+95	+66	+92	+64	+113	+42	+98	+86	+128	+65

GVHD prophylaxis	CSA/MMF	CSA/MMF	CSA/MMF	CSA/MMF	CSA/MTX	CSA/MMF	CSA/MMF	CSA/MMF	CSA/MMF	CSA/MTX	CSA/MMF	CSA/MMF	CSA/MMF	CSA/MMF	CSA/MMF
Microangiopathy (TMA)	No	No	No	No	No	No	No	No	No	No	No	No	No	No	No

Abbreviations: RD - related donor, MUD – matched unrelated donor, MMUD – mismatched unrelated donor, AML – acute myeloid leukemia, ALL – acute lymphoid leukemia, MPS – myeloproliferative syndrome, AA – aplastic anemia, CSA – Cyclosporine A, MMF – Mycophenolate mofetil, MTX – Methotrexate

Supplementary Table 3) Selected relevant pathways for cell cycle, damage and barrier function, identified by microarray analysis of sorted hepatic endothelial cells during aGVHD in the chemotherapy based LP/J→B6 model. In the first (gray) column pathways are listed. The second (orange) column shows up-regulated genes in respective pathways during aGVHD in in allo-HSCT recipients. Accordingly, numbers and example of down-regulated genes during aGVHD are displayed in the third (green) column.

Pathway		Total number of up-regulated genes and examples		Total number of down-regulated genes and examples	
Damage	Oxidative Damage	18	Bcl2, Casp3, Nfkb1	15	Cdc42, Cdkn1a,Mapk12
	FAS pathway and Stress induction of HSP regulation	22	Fasl, Casp6, Casp9	14	Fas, Hspb1, IL1a
	Complement and Coagulation Cascades	16	C2, C3, C6	31	C9, Cd59a, Vwf
	Apoptosis	48	Tnf, Casp7, Bcl2l11	34	Casp4, Casp8, Bcl2l2
	TNF-alpha NF-kB Signaling Pathway	94	Nfkbia, Bcl3, Nfkbib	72	Tnrfsf8, Nfkb2, Tnfrsf1a
Barrier function	Focal Adhesion-PI3K-Akt-mTOR-signaling pathway	107	Jak2, Angpt2, Tnc	199	Tnr, Vegfa, Vegfc
	IL-4 signaling Pathway	25	Il4, Stat5a, Dok2	29	Jak1, Mapk1, Il4ra
	Regulation of Actin Cytoskeleton	54	Mapk4, Mapk6, Actn1	91	Rhoa, Rock1, Rdx
Cell cycle	G1 to S cell cycle control	39	Cdk6, Cdk7, Cdkn2b,	14	Cdk4, Mdm2, Ccna1
	Cell cycle	56	Mcm7, Cdk2, Cdc7	17	Cdkn1a, Cdkn1b, Hdac4

Supplementary Table 4. Patient Characteristics Figure 5 panels H and M. Leukocyte infiltration as determined by CD3 and CD45 immunohistology in colon biopsies in cohort 1 of patients after alloSCT with GVHD at onset of disease vs. steroid refractory GVHD.

	Biopsy at aGVHD onset						Biopsy during SR-GVHD					
Patient Nr.	1	2	3	4	5	6	7	8	9	10	11	12
Age at alloSCT	47	11	61	28	31	52	52	45	48	48	22	49
Recipient sex	m	m	m	f	m	f	m	f	f	m	m	f
Donor sex	m	m	f	m	m	f	m	f	m	m	f	m
Donor RD MUD MMUD Haplo/MMRD/UCB	 x	 x 	 x	 x 	 x	 x	 9/10	 x	 x	 9/10	 x 	 9/10
Disease AML, MDS ALL Lymphoma, CLL MPS MM, Amyloidosis Non-malignant	AML	 FA	 HCL	 FA	 ALL	MDS	 PV/OMF	AML	AML	 MM	AML	AML
Stem cell source Peripheral blood Bone marrow	x	 x	x	x	X 2nd	x	x	x	x	x	x	x
Conditioning RIC MAC	Bu/Flu	Cy	Bu/Flu	Cy	Flu	Flu/Bu	Bu/Flu	 Cy/TBI	Bu/Flu	Treo/Flu	Flamsa	Flu/Bu
Maximum grade intestinal aGVHD	3	3	3	4	4	3	4	3	3	3	3	3
Onset of acute GVHD day post alloSCT	+61	+38	+95	+84	+121	+62	+89	+110	+41	+84	+75	+110
Biopsy taken for aGVHD day post alloSCT	+64	+45	+98	+90	+128	+65	N/A	N/A	N/A	N/A	N/A	N/A
Biopsy taken for SR-												

aGVHD day post alloSCT	N/A	N/A	N/A	N/A	N/A	N/A	+102	+123	+52	+93	+90	+132
GVHD prophylaxis medication	CSA/ MMF	CSA	CSA/ MMF	CSA/ MMF	CSA/ MMF	CSA/ MMF	CSA/ MMF	CSA/ MTX	CSA/ MMF	CSA/ MMF	CSA/ MMF	CSA/ MMF
aGVHD Therapy First line steroids (from day) Second line (drug/day of start) Third line (drug/day of start)	After Biopsy	After Biopsy	After Biopsy	After Biopsy	After Biopsy	After Biopsy	+90 ECP +97	+112 ECP +122	+42 ECP +51	+86 ECP +92	+78 ECP +86	+115 ECP +119 ATG +130
Microangiopathy (TMA)	No	No	No	No	No	No	No	No	No	No	No	No

Abbreviations: RD - related donor, MUD – matched unrelated donor, MMUD – mismatched unrelated donor, AML – acute myeloid leukemia, ALL – acute lymphoid leukemia, MPS – myeloproliferative syndrome, AA – aplastic anemia, CSA – Cyclosporine A, MMF – Mycophenolate mofetil, MTX – Methotrexate

Supplementary Table 5. Patient Characteristics Figure 5 panels I and N. Leukocyte infiltration as determined by CD3 and CD45 immunohistology in duodenum biopsies in patients after alloSCT with GVHD at onset of disease vs. steroid refractory GVHD.

	Biopsy at aGVHD onset					Biopsy during SR-GVHD				
Patient Nr.	1	2	3	4	5	6	7	8	9	10
Age at alloSCT	26	47	26	56	52	49	42	19	52	25
Recipient sex	m	f	m	f	f	m	f	m	m	f
Donor sex	m	m	m	f	f	m	f	m	m	f

Donor
  RD
  MUD
  MMUD
	
	x
	
		x
		
			x
			
				9/10
					
					x
					
						x
						
							x
							
								x
								
									9/10
										
										x

Disease
  AML, MDS
  ALL
  MPS
Non-malignant
	AML	AML	
			ALL
				MDS	MDS	
						
						CML
							MDS	
								ALL
									AML	
										
										AA

Stem cell source
  Peripheral stem cells
 	
  Bone marrow stem cells
	X
	2nd
	
		x
		
			x
			
				x
				
					x
					
						x
						
							x
							
								x
								
									x
									
										x

Conditioning
  RIC
  MAC, Aplasia conditioning
	Bu/Flu	Treo/Flu	
			Cy/TBI
				Bu/Flu	Flu/Bu	
						Cy/TBI
							
							Cy/TBI
								
								Cy/TBI
									Treo/Cy	Cy

Maximum grade intestinal aGVHD	3	3	4	3	4	3	4	3	3	4
Onset of acute GVHD day post alloSCT	+62	+88	+34	+20	+62	+55	+144	+32	+271 Post DLI	+56
Biopsy at aGVHD onset day post alloSCT	+64	+90	+37	+22	+65	N/A	N/A	N/A	N/A	N/A
Biopsy taken for SR-aGVHD day post alloSCT	N/A	N/A	N/A	N/A	N/A	+66	+158	+42	+290	+77
GVHD prophylaxis medication	CSA/MMF	CSA/MTX	CSA/MTX	CSA/MMF	CSA/ MMF	CSA/MTX	CSA/MTX	CSA/MTX	CSA/MTX	CSA/MTX

aGVHD Therapy First line steroids (from day) Second line (drug/day of start) Third line (drug/day of start)	After Biopsy	After Biopsy	After Biopsy	After Biopsy	After Biopsy	+56 ECP +63	+147 ECP +150	+32 ECP +40	+277 ECP +285	+58 ECP +65 ATG +72
Microangiopathy (TMA) No Yes (day of diagnosis)	No	No	No	No	No	No	No	No	No	No

Abbreviations: RD - related donor, MUD – matched unrelated donor, MMUD – mismatched unrelated donor, AML – acute myeloid leukemia, ALL – acute lymphoid leukemia, MPS – myeloproliferative syndrome, AA – aplastic anemia, CSA – Cyclosporine A, MMF – Mycophenolate mofetil, MTX – Methotrexate

Supplementary Table 6. Patient Characteristics Figure 5 panels J, O and P. Leukocyte infiltration and apoptotic vessels determined by CD3/CD45 immunohistology and caspase 3 staining in colon biopsies in a second cohort of patients after alloSCT with GVHD at onset of disease vs. steroid refractory GVHD. In each of these patients two biopsies were taken: Fist at onset of GVHD and the second one at diagnosis of steroid refractory GVHD.

	1	2	3	4	5	6	7	8	9	10	11
Age at alloSCT	67	69	62	54	36	43	54	29	32	30	28
Recipient sex	f	m	f	m	f	f	m	m	f	m	m
Donor sex	m	m	m	m	f	f	m	m	f	m	f
Donor RD								RD	RD		
MUD		MUD	MUD		MUD		MUD				
MMUD	MMUD			MMUD		MMUD				MMUD	
Haplo/MMRD/UCB											Haplo
Disease AML, MDS	AML		CML	MDS	MDS		AML			AML	AML
ALL						ALL			ALL		
MPS		MPS									
Non-malignant								AA			
Stem cell source Peripheral stem cells	X	X	X	X	X	X	X	X	X	X	X
Bone marrow stem cells											
Conditioning RIC	Flamsa/ATG	Flu/Bu/ATG	Flamsa/ATG	Flamsa/ATG	Flamsa/ATG		BFMT/ATG			Flamsa/ATG	
MAC, Aplasia conditioning						Eto/Cy/TBI/ ATG		Bu/Cy/ATG	Eto/Cy/TBI		Flu/Bu/ Thiotepa
Maximum grade intestinal aGVHD	4	4	4	4	4	4	2-3	2-3	4	4	4
Onset of acute GVHD day post alloSCT	+25	+61	+35	+104	+21	+24	+17	+48	+26	+22	+19
Biopsy taken for aGVHD day post alloSCT	+25	+61	+35	+106	+30	+141	+109	+140	+26	+20	+19
Biopsy taken for SR-	+39	+68	+69	+121	+51	+160	+126	+158	+43	+45	+50

aGVHD day post alloSCT											
GVHD prophylaxis medication	CSA/MMF	CSA/MMF	CSA/MMF	CSA/MMF	CSA/MMF	CSA/MMF	CSA/MMF	CSA/MTX	CSA/MMF	CSA/MMF	CSA/MMF/Cy
aGVHD Therapy First line steroids (from day) Second line (drug/day of start) Third line (drug/day of start)	+25 Ruxolitinib +34 Infliximab +41	+58 Infliximab +68 MSC +146	+35 Infliximab +78 na	+105 Infliximab +114 na	+30 Infliximab +37 Ruxolitinib +85 MSC +141	+141 Infliximab +161 MSC +183	+110 Ruxolitinib +133 na	+140 Infliximab +145 Ruxolitinib +193(konsolid.)	+27 Simulect +33 Infliximab +57	+31 Infliximab +46 Ruxolitinib +113	+15 Infliximab +50
Microangiopathy (TMA)	no	no	no	no	no	no	no	no	Suspected 04/2014	Yes 02/03/2015	no

Abbreviations: RD - related donor, MUD – matched unrelated donor, MMUD – mismatched unrelated donor, AML – acute myeloid leukemia, ALL – acute lymphoid leukemia, MPS – myeloproliferative syndrome, AA – aplastic anemia, CSA – Cyclosporine A, MMF – Mycophenolate mofetil, MTX – Methotrexate